JOURNAL OF AGRICULTURAL AND FOOD CHEMISTRY
ARTICLE

J. Agric. Food Chem. 2009, 57, 4091–4095 4091
DOI:10.1021/jf9000605

Quantitative ^{23}Na Magnetic Resonance Imaging of Model Foods

Emil Veliyulin,*,† Bjørg Egelandsdal,‡ Florin Marica,§ and Bruce J. Balcom§

†SINTEF Fisheries and Aquaculture, N-7465 Trondheim, Norway, ‡Department of Chemistry, Biotechnology and Food Science, Norwegian University of Life Science, N-1432 Ås, Norway, and §MRI Centre, Department of Physics, University of New Brunswick, Fredericton NB, Canada E3B 5A3

Partial ^{23}Na MRI invisibility in muscle foods is often referred to as an inherent drawback of the MRI technique, impairing quantitative sodium analysis. Several model samples were designed to simulate muscle foods with a broad variation in protein, fat, moisture, and salt content. ^{23}Na spin−echo MRI and a recently developed ^{23}Na SPRITE MRI approach were compared for quantitative sodium imaging, demonstrating the possibility of accurate quantitative ^{23}Na MRI by the latter method. Good correlations with chemically determined standards were also obtained from bulk ^{23}Na free induction decay (FID) and CPMG relaxation experiments on the same sample set, indicating their potential use for rapid bulk NaCl measurements. Thus, the sodium MRI invisibility is a methodological problem that can easily be circumvented by using the SPRITE MRI technique.

KEYWORDS: Sodium; MRI; salting; SPRITE; quantification

INTRODUCTION

Salting of muscle foods is an important food preservation method. There are several major salting techniques that have been developed based on tradition. Evaluation of the quality of salted products is often made on the basis of long experience and food traditions in a particular country or region. Analytical determination of the salt content in muscle foods is usually made using destructive techniques (*1*−*7*), but there is increasing interest in rapid, noninvasive, and nondestructive methods allowing measurement of the salt content.

Magnetic resonance imaging (MRI) is an imaging technique that offers a unique opportunity to noninvasively study intact objects, producing high quality cross-section images of biological systems. There are a number of examples where MRI has been applied to study the chemical and physical properties, anatomical structure and dynamic processes in foods (*8*, *9*). Proton (^{1}H) MRI is the most used modality allowing differentiation of protons in molecules with different mobility or chemical environment. Using a variety of ^{1}H MRI protocols, images differentiating water from fat (*10*) or connective tissue (*11*) as well as images to track diffusion (*12*) have been demonstrated.

Qualitative sodium MRI has been used to study the distribution of brine in rabbit muscle (*13*) and cod fillets (*14*). Quantitative ^{23}Na MRI has, however, been problematic because of a well-known partial salt invisibility phenomenon reported earlier (*15*, *16*). Partial sodium NMR invisibility arises from the quadrupolar interactions of the sodium bound to macromolecules and other restricted or structured sodium molecules, which results in extremely short ^{23}Na NMR relaxation components, virtually unobservable in spin−echo MRI experiments and often interpreted as a loss of sodium signal. The feasibility of obtaining quantitative information about the sodium content using ^{23}Na NMR relaxometry was demonstrated in a comparative study of salting and desalting of cod (*14*). In the experiment, CPMG T_2 relaxation curves were acquired from salted cod samples and reference brines, and the initial amplitudes were used to calculate the NaCl content in the unknown cod samples. The authors found good correlation between the total salt content determined chemically and by the NMR technique. This indicated that the relatively long echo times used for detection in spin−echo MRI experiments are the most probable reason for the partial MRI sodium invisibility. Recently, ^{23}Na spin density maps of the human brain were obtained using a single-point ramped imaging with T_1 enhancement (SPRITE) MRI technique (*17*). This technique uses free induction decay (FID) signals that allow the detection of very short relaxation times that are normally missed in spin−echo techniques. Proton SPRITE, being a pure phase encoding technique, has been successfully applied for imaging of a wide range of materials with short MRI signal lifetimes, such as sedimentary rocks, concrete (*18*), and various gases (*19*).

Producing quantitative MRI images in practice requires complete recovery of the amplitudes of the FID signals constituting the *k*-space used for the image reconstruction. To achieve this, both the T_1 and T_2* weighting effects in the images must be maximally reduced. T_1 weighting can be practically avoided by selecting the repetition time of the MRI experiment at least three times longer than the longest relaxation component present in the sample. T_2* weighting is practically difficult to avoid, and MR images are usually to a certain extent either T_2 or T_2* weighted. Signal acquisition in SPRITE MRI is based on the detection of the free induction decay (FID) signal, which theoretically means that the SPRITE MRI signal can be detected as early as the dead time of the instrument allows, thus effectively minimizing T_2* weighting in the images.

*Corresponding Author. Phone: (+47) 982 45 035. Fax: (+47) 932 70 701. E-mail: emil.veliyulin@sintef.no.

 Published on Web 4/20/2009

In this work, the applicability of the ^{23}Na SPRITE MRI method for quantitative sodium imaging is investigated. The results are compared with those obtained by a spin−echo protocol as well as bulk NMR measurements using FID and CPMG techniques on the same sample set. The model meat samples studied have salt concentrations and chemical compositions normally encountered in the production of dry cured ham.

MATERIALS AND METHODS

Samples. Thirteen model samples were designed to simulate homogenized muscle foods with a broad variation in the protein, fat, moisture, and salt content. Eleven samples were made using thoroughly ground semimembranosus pork muscle, powdered dried muscle, ground pork back fat, water, and fine NaCl salt. These samples were taken from a larger set of model samples used in a computed tomography study (*20*), in which a detailed description of the sample design can be found. The meat ingredients used here have been frozen and freeze-dried during sample preparation as described in ref *20*. In addition, two frozen and thawed minced samples of brine salted cod, each from a separate fillet, were included in the study. The fillets were pickle salted for one week and then dry salted for an additional week. The first sample was prepared by mincing a white muscle piece cut from the original salted fillet. The second fillet was rehydrated in water overnight at 4 °C prior to mincing. All studied model samples were minces made out of frozen−thawed or freeze-dried ingredients, and therefore, the original structure of the intact fresh muscle was disrupted during sample preparation. Thus, frozen storage of the samples between the two experimental series could not make any significant additional changes in their microstructure.

^{23}Na MRI Measurements. The spin−echo ^{23}Na MRI studies were carried out on a Bruker Avance AV300 instrument (Bruker BioSpin GmbH, Ettlingen, Germany) with a magnetic field strength of 7 T and horizontal bore opening using a commercial ^{1}H/^{23}Na double tuned 72 mm Birdcage probe. The temperature inside the probe was about 15 °C. A multislice multiecho imaging protocol (MSME) with the following parameters was applied: one slice image with 10 mm thickness was acquired; matrix size (MS) = 128 × 128; number of scans (NS) = 64; field of view (FOV) = 9 cm; and relaxation delay (RD) = 200 ms. Eight successive echoes with an echo time (τ) of 6.1 ms were acquired, and the total experimental time was about 14 min. In the experiment, a cylindrical Plexiglas sample holder (100 mm length, 60 mm diameter) with a separate chamber for the internal reference was used. The concentration of the reference brine was 6%.

SPRITE ^{23}Na MRI experiments were performed on a MARAN spectrometer (Resonance Instruments Ltd., Oxford, UK) with a 7 T, wide bore, horizontal superconducting magnet 7 T/60/AS (Magnex Scientific Ltd., Oxford, UK) using a homemade 62 mm inner diameter ^{23}Na RF probe. The standard microimaging gradient set SGRAD156/100/S (Magnex Scientific Ltd., Oxford, UK) employed was powered by a set of three Techron 7782 gradient amplifiers (Elkhart, Indiana, USA), providing a maximum gradient strength of 38 G/cm. The measurements were carried out at 11 °C inside the probe.

A special rectangular Plexiglas sample holder (60 × 35 × 35 mm) was designed for the SPRITE measurements with a sample chamber (in plane size 35 × 40 mm) and two cylindrical openings for the reference solutions (10 mm diameter). The reference brines had concentrations of 5 and 10%. The minces were carefully pressed into the sample chamber avoiding air bubble trapping. The filling height for the samples and the reference brines was 20 mm. Weights of all imaged samples were recorded as well. Nonslice selective SPRITE images of each sample were taken with the encoding times of 0.12, 0.5, 1, 1.5, 2, 2.5, 3, 3.5, 4, 4.5, 5, 6, 8, and 10 ms, acquiring 4 k-space spiral trajectories with a separation time RD = 2 s. The gradient stabilization time was set to 1.5 ms. The other experimental parameters were MS = 64 × 64, NS = 64, and FOV = 10 cm. All homogenized model samples were stored frozen between the two MRI studies for about 1 month and homogenized once more prior to the second MRI study.

CPMG and FID Measurements. In addition to imaging, ^{23}Na relaxation measurements were performed on the same set of minced samples using CPMG (*21*, *22*) and free induction decay (FID) techniques (*23*). The same magnet as for the SPRITE MRI investigations was used for these measurements. Minced samples were weighed (≈20 g) in small plastic bags, placed in the iso-center of the magnet, and CPMG and FID curves were measured. The acquisition parameters for the CPMG experiment were echo time = 0.6 ms, RD = 2 s, and NS = 64. Depending on the sample's relaxation properties, either 128 or 256 echoes were recorded to achieve complete relaxation of the echo train. The FIDs were recorded with RD = 2 s and NS = 64, acquiring 2048 points. For quantification purposes, two reference brines (5 and 10%) were weighed in glass vials and separately measured with identical protocols.

Data Analysis. All data processing was made with in-house software using the Interactive Data Language (IDL version 5.5, ITT VIS, New York, USA). Regions of interest (ROI) covering most of the object (avoiding the edges) were drawn in the samples, and the mean intensities in the ROI were calculated for each encoding time t_p (SPRITE) and accumulated echo times $t_n = n\tau$ (spin−echo). For the reference brines in the SPRITE MRI images, only the pixels with highest intensity were chosen because of the relatively small reference sample sizes and strong edge effects.

The local image intensity S_{MSME} of the spin−echo MRI experiment was fit to the following monoexponential expression (*24*):

$$S_{MSME} = S^0{}_{MSME} \cdot \exp\left(-\frac{t_n}{T_2}\right) + N \quad (1)$$

where S^0_{MSME} is the initial amplitude of the sodium signal, T_2 is the transversal relaxation time, and N is noise in the images. For SPRITE experiments, the corresponding equation for the intensity S_{SPRITE} is

$$S_{SPRITE} = S^0{}_{SPRITE} \cdot \exp\left(-\frac{t_p}{T_2{}^*}\right) \sin\Theta + N \quad (2)$$

where t_p is the encoding time, Θ is the RF pulse flip angle, and T_2* is the effective transversal relaxation time (*25*). The noise N was calculated in each set of images. Only the encoding times up to 5 ms were used for curve fitting due to the low signal-to-noise ratio at longer t_p. Using the fitted amplitudes of the sodium signal for the samples S^0_{sample} and the reference brines S^0_{ref}, sodium content in the samples was determined as

$$C_{sample} = C_{ref} \cdot \frac{S^0{}_{sample}}{S^0{}_{ref}} \quad (3)$$

Equal heights of the imaged samples and the references allowed such a simple calculation procedure. In the slice-selective spin−echo MRI method, the height was determined by the slice thickness of the image, while in the SPRITE experiments all samples had equal filling height in the holder. Typical T_1 relaxation time values of ^{23}Na nuclei in biological materials are about 30 ms (*26*). No correction for the longitudinal relaxation was made because of the sufficiently long waiting time between acquisitions of the successive k-space trajectories in both SPRITE and spin−echo experiments (RD > $5T_1$).

For the FID experiment, the sodium signal amplitudes for the samples and the reference brines were determined using an expression similar to eq 2. The calculated sodium signals were then normalized with the sample weights, and a calibration line through three points was drawn (5 and 10% references and the noise). Using this calibration, the sodium content for all samples was determined.

CPMG data were analyzed by fitting of the experimental relaxation curve to a double exponential model, following ref *27*:

$$S_{CPMG} = S_1 \cdot \exp\left(-\frac{t}{T_2{}^1}\right) + S_2 \cdot \exp\left(-\frac{t}{T_2{}^2}\right) + N \quad (4)$$

where S_1 and S_2 are amplitudes of the two sodium relaxation components present in the samples, while T_2^1 and T_2^1 are their respective transverse relaxation times. The two relaxation times represent the slow and the fast relaxation components as suggested in ref *27*.

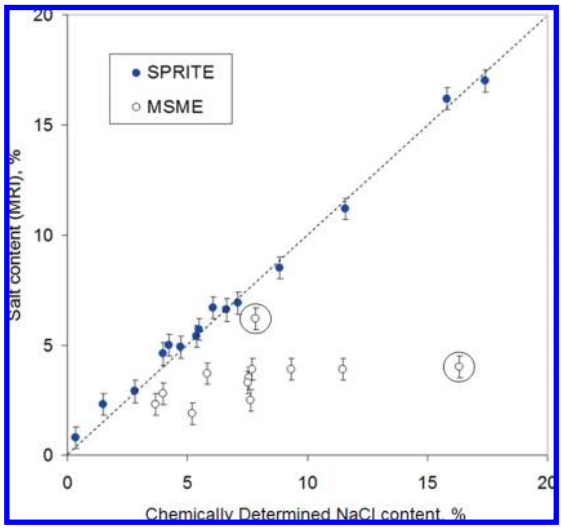

Figure 1. Correlation of the salt content determined from the SPRITE and spin−echo MRI protocols with the data measured chemically.

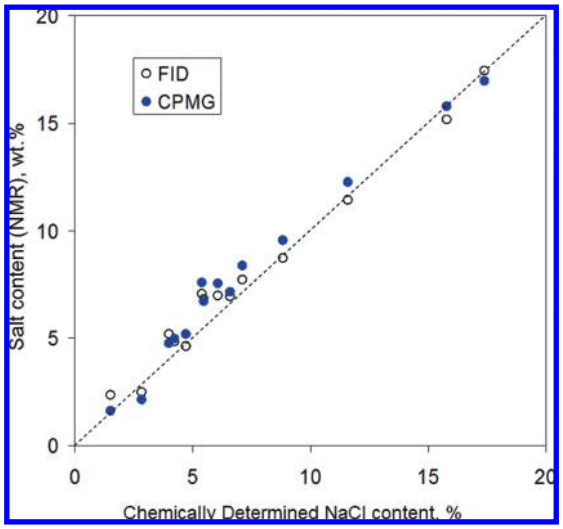

Figure 2. Sodium content calculated from the bulk FID and CPMG measurements plotted against the corresponding chemically determined NaCl content. Sodium content calculated from the bulk FID and CPMG measurements plotted against the corresponding chemically determined NaCl content.

Chemical Analysis. Salt content determined from the MR images was correlated with either that determined by the reference chemical method or calculated from the sample preparation. Each mince investigated by MRI was additionally homogenized and the salt content (~5 g homogenates) was analyzed using the Vollhard method (*28*) on two parallel samples. The protein content in the samples was determined using the Kjeldahl method (*29*).

RESULTS AND DISCUSSION

Correlation of the salt contents determined from the SPRITE and the spin−echo MRI modalities with the chemically determined values are shown in the **Figure 1**. From the last figure, it is obvious that the spin−echo MRI technique strongly underestimates the salt content, demonstrating partial MRI salt invisibility. Sodium MRI visibility coefficients were estimated as ratios of the MRI-calculated salt contents in the samples to those determined chemically. The worst underestimation of the salt content (visibility coefficient 0.25) is observed for the most salted sample (16.3%; circled in **Figure 1**), while the sample with 7.8% salt showed the highest sodium visibility (0.79; circled in **Figure 1**). A negative correlation (R^2 = 0.71) between the spin−echo MRI visibility coefficient and the protein content in the samples (known from the sample preparation) supports the hypothesis that the bound part of the sodium is residing on the protein sites. This is in agreement with an observation made for cod and salmon fillet pieces salted at different concentrations (*29*). For SPRITE MRI data, correlation with the chemically determined NaCl content was much better than that for spin−echo MRI. A root-mean-square error of prediction (RMSEP) equal to 0.4% NaCl was calculated for all studied samples (n = 15, 13 model meat samples and 2 fish samples) from the SPRITE MRI data in the **Figure 1**. The 13 model meat samples represented a subset of a larger sample set examined by computer tomography (CT) using the methodology described by Håseth et al. (*20*). The 13 common meat samples between the two studies showed a RMSEP of 0.4% NaCl for SPRITE MRI and a RMSEP of 1.7% NaCl for the CT.

Table 1. Short and Long Relaxation Times Calculated from the Bulk CPMG Measurement and the Ratio of Their Corresponding Amplitudes

sample	T_2^1 (ms)	T_2^2 (ms)	A^1/A^2
1	3.7	17.0	1.3
2	4.3	30.2	0.4
3	1.2	6.3	3.5
4	4.0	29.1	0.5
5	1.7	10.5	2.0
6	1.2	7.6	2.2
7	3.9	27.3	0.8
8	2.5	15.4	1.5
9	3.0	17.7	2.0
10	3.3	17.3	2.2
11	2.4	17.1	1.7
12	2.2	14.5	1.6
13	4.4	17.5	1.6
14	1.5	13.7	1.8
15	4.8	22.8	2.0

Sodium content in the samples calculated from the bulk FID and CPMG measurements are plotted in **Figure 2** against the corresponding chemical data, demonstrating good correspondence of the NMR results with the reference chemical method, indicating total ^{23}Na NMR visibility.

Table 1 summarizes the relaxation times of the two components and their amplitude ratio obtained by fitting of the double-exponential model to bulk CPMG relaxation curves. Large variability between the samples in both relaxation times and the amplitude ratio A^1/A^2 indicate that the ^{23}Na NMR relaxation properties of muscle foods depended on their chemical composition in a complex manner. Upon plotting A^1/A^2 values against the corresponding protein contents of the samples (**Figure 3**), a strong correlation (R^2 = 0.8) was observed, additionally suggesting that the sodium ions with the short relaxation times were mainly associated with the protein molecules. Quantification of the bound sodium fraction can be performed using double-quantum filtered NMR spectroscopy (*30*), and it would be interesting to compare the A^1/A^2 ratios reported here with the bound sodium fraction measured in this way.

These results indicate that the partial MRI sodium invisibility observed in the spin−echo experiment can be explained by the inability to observe most of the rapidly relaxing ^{23}Na component due to the relatively long echo time (6.1 ms) of the multislice multiecho imaging protocol, which was the shortest possible echo time due to the timing limitations of this MRI sequence. This conclusion was further supported by the negative correlation (R^2 = 0.75) between the spin−echo MRI visibility coefficients

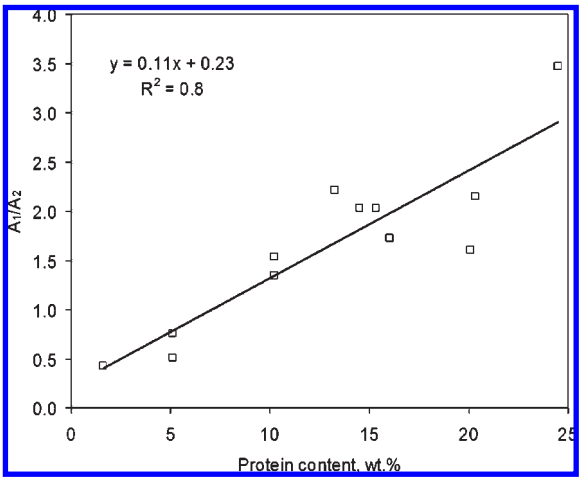

Figure 3. Ratio of the amplitudes of the short/long relaxation components measured by CPMG ^{23}Na NMR (A^1/A^2 in **Table 1**) vs the measured protein content in the samples.

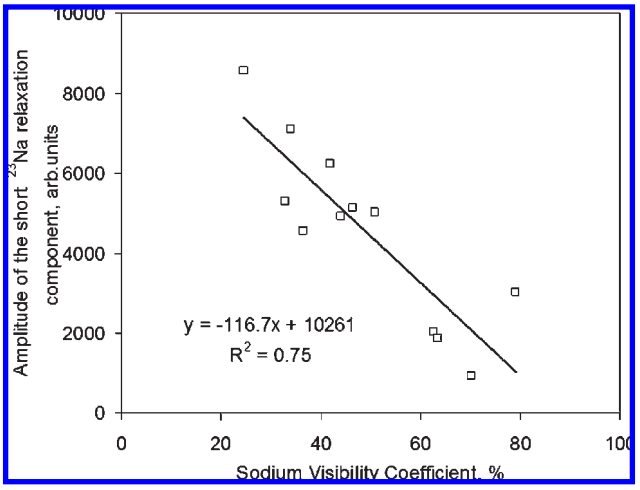

Figure 4. Amplitude of the short relaxation component of the CPMG ^{23}Na MRI signal vs the calculated spin−echo MRI sodium visibility coefficient.

and the corresponding amplitudes of the short relaxation component for the studied samples shown in **Figure 4**.

To summarize the main results of this article, one has to mention that the salt contents in the investigated samples determined from the spin−echo MRI technique were underestimated to various degrees (up to 75%) in most samples, while four almost liquid model samples showed no sodium underestimation, within experimental errors. Sodium content determined from the SPRITE MRI images showed good correlation with the corresponding chemical measurements of NaCl content (R^2 = 0.995), thus demonstrating the applicability of the SPRITE imaging approach for quantitative sodium analysis in muscle foods. Results of the FID and CPMG bulk measurements on the same sample set showed good correspondence with the chemical data as well. The noninvasive and nondestructive nature of the MRI approach makes the SPRITE MRI technique attractive for optimization of salting processes in food research and industry, when knowledge of the salt distribution is important. If only the total NaCl content needs to be measured, bulk relaxation measurements (FID or CPMG) can be used for a more rapid measurement than chemical analysis.

LITERATURE CITED

(1) Jason, A. C. Effects of fat content on diffusion of water in fish muscle. *J. Sci. Food Agric.* **1965**, *16*, 281–288.

(2) Sannaveerappa, T.; Ammu, K.; Joseph, J. Protein-related changes during salting of milkfish (*Chanos chanos*). *J. Sci. Food Agric.* **2004**, *84*, 863–869.

(3) Thorarinsdottir, K. A.; Arason, S.; Bogason, S. G.; Kristbergsson, K. The effects of various salt concentrations during brine curing of cod. *Int. J. Food Sci. Technol.* **2004**, *39*, 79–89.

(4) Wang, D.; Tang, J.; Correia, L. R. Salt diffusivities and salt diffusion in farmed Atlantic salmon muscle as influenced by rigor mortis. *J. Food Eng.* **2000**, *43*, 115–123.

(5) Rørå, A. M.; Furuhaug, R.; Fjæra, S. O.; Skjervold, P. O. Salt diffusion in pre-rigor filleted Atlantic salmon. *Aquaculture* **2004**, *232*, 255–263.

(6) Gallart-Jornet, L.; Barat, J. M.; Rustad, T.; Erikson, U.; Escriche, I.; Fito, P. A comparative study of brine salting of Atlantic cod (*Gadus morhua*) and Atlantic salmon (*Salmo salar*). *J. Food Eng.* **2007**, *79*, 261–270.

(7) Gallart-Jornet, L.; Barat, J. M.; Rustad, T.; Erikson, U.; Escriche, I.; Fito, P. Influence of brine concentration on Atlantic salmon fillet salting. *J. Food Eng.* **2007**, *80*, 267–275.

(8) Martinez, I.; Aursand, M.; Erikson, U.; Singstad, T. E.; Veliyulin, E.; van der Zwaag, C. Destructive and non-destructive analytical techniques for authentication and composition analyses of foodstuffs. *Trends Food Sci. Technol.* **2003**, *14*, 489–498.

(9) Ruan, R. R.; Chen, P. L. Nuclear Magnetic Resonance Techniques and Their Application in Food Quality Analysis. In *Nondestructive Food Evaluation*; Gunasekaran, S., Ed.; Marcel Dekker Inc.: New York, 2001; pp 165−216.

(10) Tingle, J. M.; Pope, J. M.; Baumgartner, P. A.; Sarafis, V. Magnetic resonance imaging of fat and muscle distribution in meat. *Int. J. Food Sci. Technol.* **1995**, *30*, 437–446.

(11) Bonny, J. M.; Laurent, W.; Renou, J. P. Characterisation of Meat Structure by NMR Imaging at High Field. In *Magnetic Resonance in Food Science: A View to the Future*; Webb, G. A., Ed.; Royal Society of Chemistry: Cambridge, U.K., 2001; pp 17−21.

(12) Mulkern, R. V.; Spencer, R. G. S. Diffusion imaging with paired CPMG sequences. *Magn. Reson. Imaging* **1988**, *6*, 623–631.

(13) Renou, J. P.; Benderbous, S.; Bielicki, G.; Foucat, L.; Donnat, J. P. ^{23}Na Magnetic Resonance Imaging: distribution of brine in muscle. *Magn. Reson. Imaging* **1994**, *12*, 131–137.

(14) Erikson, U.; Veliyulin, E.; Singstad, T.; Aursand, M. Salting and desalting of fresh and frozen-thawed cod (*Gadus morhua*) fillets: A comparative study using ^{23}Na NMR, ^{23}Na MRI, low-field ^{1}H NMR and physicochemical analytical methods. *J. Food Sci.* **2004**, *69*, E107–E114.

(15) Springer, C. S. Measurement of metal cation compartmentalization in tissue by high-resolution metal cation NMR. *Ann. Rev. Biophys. Chem.* **1987**, *16*, 375–399.

(16) Shapiro, E. M.; Borthakur, A.; Dandora, R.; Kriss, A.; Leigh, J. S.; Reddy, R. Sodium visibility and quantitation in intact bovine articular cartilage using high field ^{23}Na MRI and MRS. *J. Magn. Reson.* **2000**, *142*, 24–31.

(17) Romanzetti, S.; Halse, M.; Kaffanke, J.; Zilles, K.; Balcom, B. J.; Shah, N. J. A comparison of three SPRITE techniques for the quantitative 3D imaging of the ^{23}Na spin density on a 4T whole-body machine. *J. Magn. Reson.* **2006**, *179*, 56–64.

(18) Chen, Q.; Halse, M.; Balcom, B. J. Centric scan SPRITE for spin density imaging of short relaxation time porous materials. *Magn. Reson. Imaging* **2005**, *23*, 263–266.

(19) Prado, P. J.; Balcom, B. J.; Mastikhin, I. V.; Cross, A. R.; Armstrong, R. L.; Logan, A. Magnetic resonance imaging of gases: A single-point ramped imaging with T_1 enhancement (SPRITE) study. *J. Magn. Reson.* **1999**, *137*, 324–332.

(20) Håseth, T. T.; Egelandsdal, B.; Bjerke, F.; Sørheim, O. Computed tomography for quantitative determination of sodium chloride in ground pork and dry-cured hams. *J. Food Sci.* **2007**, *72*, E420–E427.

(21) Carr, H. Y.; Purcell, E. M. Effects of diffusion on free precession in nuclear magnetic resonance experiments. *Phys. Rev.* **1954**, *94*, 630–638.

(22) Meiboom, S.; Gill, D. Modified spin-echo method for measuring nuclear relaxation times. *Phys. Rev.* **1958**, *29*, 688–691.

(23) Farrar, T. C.; Becker, E. D. *Pulse and Fourier Transform NMR*; Academic Press Inc.: London, U.K., 1971; pp 19−25.
(24) Veliyulin, E.; Aursand, I. G. ^{1}H and ^{23}Na MRI studies of Atlantic salmon (*Salmo salar*) and Atlantic cod (*Gadus morhua*) fillet pieces salted in different brine concentrations. *J. Sci. Food Agric*. **2007**, *87*, 2676–2683.
(25) Halse, M.; Goodyear, D. J.; MacMillan, B.; Szomolanyi, P.; Matheson, D.; Balcom, B. J. Centric scan SPRITE magnetic resonance imaging. *J. Magn. Reson*. **2003**, *165*, 219–229.
(26) Kim, R. J.; Lima, J. A.; Chen, E. L.; Reeder, S. B.; Klocke, F. J.; Zerhouni, E. A.; Judd, R. M. Fast ^{23}Na magnetic resonance imaging of acute reperfused myocardial infarction. Potential to assess myocardial viability. *Circulation* **1995**, *95*, 1877–1885.
(27) Bertram, H. C.; Holdsworth, S. J.; Whittaker, A. K.; Andersen, H. J. Salt diffusion and distribution in meat studied by ^{23}Na nuclear magnetic resonance imaging and relaxometry. *J. Agric. Food Chem*. **2005**, *53*, 7814–7818.
(28) Association of Official Analytical Chemists. *Official Methods of Analysis*, 15th ed.; Vol. *2*; AOAC: Arlington, VA, 1990; p 810.
(29) Association of Official Analytical Chemists. AOAC Official Method 981.10 Crude Protein in Meat: Block Digestion Method. In *Official Methods of Analysis of AOAC, International* 16th ed., 4th rev.; AOAC International: Gaithersburg, MD, pp. 7−8, 1999.
(30) Mouaddab, M.; Foucat, L.; Donnat, J. P.; Renou, J. P.; Bonny, J. M. Absolute quantification of Na^{+} bound fraction by double-quantum filtered ^{23}Na NMR spectroscopy. *J. Magn. Reson*. **2007**, *189*, 151–155.

Received for Review July 8, 2008. Revised manuscript received March 16, 2009. Accepted April 01, 2009. Financial support of The Research Council of Norway through the strategic institute program "Production improvements of salted/cured meat and fish: development of rapid and non-destructive salt analyses related to production and quality" (NFR project no. 153381/140) is greatly acknowledged. B.J.B. thanks NSERC for a Discovery grant and the Canada Chairs program for a Research Chair in MRI of materials. The UNB MRI Centre is supported by an NSERC Major Facilities Access Award.